Demonstration of semiconductor characterization by phonon sidebands in photoluminescence

D. C. Reynolds and D. C. Look
University Research Center, Wright State University, Dayton, Ohio 45433

D. N. Talwar,* G. L. McCoy, and K. R. Evans
Solid State Electronics Directorate (WL/ELRA), Wright Laboratories, Wright Patterson Air Force Base, Ohio 45433-6543
(Received 10 August 1994)

In this paper two GaAs samples were investigated; one was a very pure sample grown by chemical-vapor deposition, the other was grown by molecular-beam epitaxy. The dominant optical transition in the high-purity sample was the donor-bound-exciton transition. Phonon sidebands associated with both the free exciton and the donor-bound exciton were observed. The active phonons were the longitudinal-optical (LO) and the transverse-optical (TO) modes associated with both the free exciton and the donor-bound exciton at the Γ point in $\mathbf{k}$ space; the TO mode from the donor-bound exciton at the X point, the LO from the free exciton at the L point and/or X point, and the longitudinal-acoustical mode from the free exciton at the X point and the L point. These phonon-coupled exciton transitions were not observed in the sample grown by molecular-beam epitaxy; however, phonon sidebands associated with free-to-bound and bound-to-bound transitions were observed. The transverse-acoustical mode at the X point was observed along with lower-energy modes that were attributed to impurity and defect structures in the material.

I. INTRODUCTION

Phonon sidebands have been observed in the optical transitions of many materials. From these measurements intrinsic bulk phonon energies can be determined as well as impurity-related phonon energies. In materials where the phonon-dispersion relations are known, the phonon sidebands can reveal phonon modes throughout the zone. In the case of GaAs, phonon modes have been determined from different experimental techniques. Lattice absorption measurements in the $10-40\mu$ range were used to establish five different phonon energies.[1] These, along with the known elastic constants, allowed a calculation of the complete phonon spectrum using an extension of the shell model. An 11-parameter rigid-ion model was later used to describe the lattice dynamics of GaAs.[2] The calculated frequencies were compared with those obtained from other models and were also compared to measured neutron-scattering data.[3,4] The model was also extended to compare with data obtained from second-order Raman spectra.[5]

In the current experiment the host material was unintentionally doped GaAs. Two samples were investigated: one was a very pure layer grown by chemical vapor deposition (CVD), while the other, somewhat less pure, was grown by molecular beam epitaxy (MBE). The dominant optical feature in the high-purity sample was the donor bound exciton (D^0,X) transition, and all other transitions were less intense by at least an order of magnitude. In this sample phonon sidebands associated with both the free exciton (X) and D^0,X were observed; in fact, the phonons appeared to couple more strongly to X than to D^0,X. The phonons that were observed in this sample were the LO from both X and D^0,X at the Γ point, the TO from both X and the D^0,X at the Γ point, the TO from D^0,X at the X point, the LO from the X at the L and/or X point, the LA from X at the X point, and the LA from X at the L point. In almost all cases the phonon sidebands were very sharp and were identified from the phonon dispersion relations of Waugh and Dolling.[3] In all cases the emission of the LO-phonon-coupled lines was more intense than that of TO-coupled lines. This is expected from the results of Frölich and Mott,[6] who showed that electrons moving in a crystal interact mainly with the longitudinal-optical vibrations if the polar forces are sufficiently large.

None of the above phonon-coupled transitions were observed in the MBE-grown sample. However, in this sample phonon side bands were observed from the free to bound F-B (free electron to bound hole) and bound to bound B-B (bound electron to bound hole) transitions. The transverse acoustical (TA) mode at the X point was observed along with the lower-energy phonons which were attributed to impurity and defect structure in the material. When the pump energy is resonant with the more intense regions of the F-B and B-B transitions, the LO and TO modes are also observed.

The observation of phonon sidebands is a technique that can be used to assess material quality. In high-quality samples, intrinsic phonon modes at different points in the zone are observed. When the impurity content of the sample increases, these modes disappear and modes associated with impurity and defect structure appear.

II. EXPERIMENTAL DETAILS

The very high-purity sample used in this study was epitaxially grown on a semi-insulating (SI) GaAs:Cr substrate by means of the H_2:$AsCl_3$:Ga vapor deposition

technique. Hall and electrical conductivity measurements were used to characterize the electrical parameters of the sample. The electron mobility of the sample was 1.4×10^5 cm^2/V sec at 77 K, and the total concentration of electrically active impurities was 1.3×10^{14} cm^{-3}. The sample of lower purity was grown by solid source molecular-beam epitaxy (As_2 species) in a commercial MBE chamber which is used extensively for device production, and this is expected to produce higher than usual quantities of background impurities. The sample was grown on a SI GaAs(001) substrate and consisted of an $Al_xGa_{1-x}As$/GaAs superlattice buffer followed by 5000 Å of nominally undoped GaAs followed by an $Al_xGa_{1-x}As/In_xGa_{1-x}As$/GaAs pseudomorphic high electron mobility (*p*HEMT) device structure. The undoped GaAs from this MBE typically is *n* type, with a carrier concentration of $\sim10^{15}$ cm^{-3} and a mobility of 6×10^4 cm^2/V sec at 77 K.

The photoluminescence (PL) spectra were excited with an Ar^+-ion laser pumped tunable dye laser using styryl 9 dye. The measurements were made at 2 K with the sample immersed in liquid He. The spectra were analyzed with a high-resolution 4-m spectrometer equipped with a RCA C31034A photomultiplier tube for detection.

III. EXPERIMENTAL RESULTS

The emission spectra from the sample grown by chemical vapor deposition are shown in Fig. 1. The dominant transition is the D^0,X transition, with all other transitions very much reduced in intensity. The free exciton transition is observed along with rotator states associated with D^0,X. The free to bound transition in this case is the free hole to bound electron. The $J=\frac{3}{2}$ and $J=\frac{5}{2}$ states of the acceptor bound exciton (A^0,X) are also observed along with the $n=2$ state of D^0,X. Not shown is the spectral region where the *F-B* and *B-B* transitions would normally be observed; however, at the detector sensitivity setting for Fig. 1 these transitions are not observed.

The phonon sidebands associated with the emission spectra in Fig. 1 are shown in Fig. 2. Pumping resonantly at the free exciton energy produces the phonon sidebands shown as the solid curve, while pumping resonantly at the D^0,X energy produces the spectra shown as the dashed curve. It is clear that most phonons are more strongly coupled to the free exciton than to the bound exciton. The phonon sidebands are labeled with their appropriate positions in the zone. The phonon energies, as determined from the transition energies are given in Table I. The energies are in very good agreement with those given in Ref. 3.

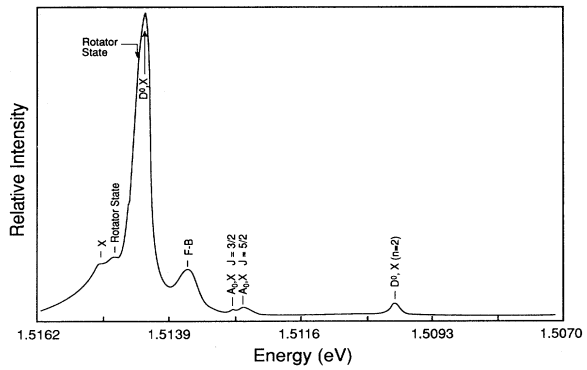

FIG. 1. Emission spectra from the high-purity GaAs sample grown by chemical-vapor deposition.

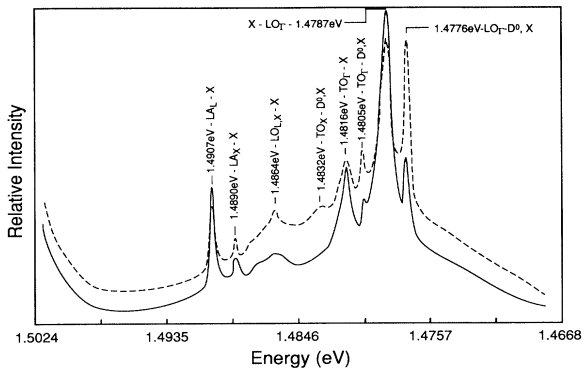

FIG. 2. Phonon sidebands associated with the emission spectra from Fig. 1. Solid line: pump energy resonant with *X*; dashed line: pumping at D^0,X energy.

The emission spectra from the sample grown by MBE are shown in Fig. 3. The dominant transition is the free exciton transition, with D^0,X being slightly less intense and A^0,X considerably less intense. The *F-B* and *B-B* transitions are readily observable with peak intensities approximately half that of the free exciton. Phonon replicas associated with exciton-related transitions were not observed; however, phonon replicas associated with transitions in the *F-B* and *B-B* spectral region were observed. Phonon replicas observed with a pump energy of 1.4855 eV, which is on the long-wavelength tail of the *B-B* transition, are shown in Fig. 4. The transition at 1.4835 eV which gives a phonon energy of 2.0 meV is still not identified. It is likely that the mode is related to a complex center involving In_{Ga} (cf. Sec. IV).

The transition at 1.4816 eV has been identified as an in-band resonant mode of indium occupying the gallium site (In_{Ga}). Although the sample was not intentionally doped there is an In oven incorporated into the system for growing In-related compounds. Therefore, indium is most likely a residual from the system. The transition at 1.4798 eV is identified with the Ga vacancy (V_{Ga}). The transition at 1.4753 eV results from the transverse-acoustical (TA) phonon at the *X* point. The phonon repli-

TABLE I. Phonon replicas observed at the Γ, *X*, and *L* points in *k* space along with their associated energies.

Phonon replica	Γ (meV)	*X* (meV)	*L* (meV)
X-LO	36.6	28.9	28.9
D^0,X-LO	36.8		
X-TO	33.7		
D^0,X-TO	33.9	31.2	
X-LA		26.3	24.6

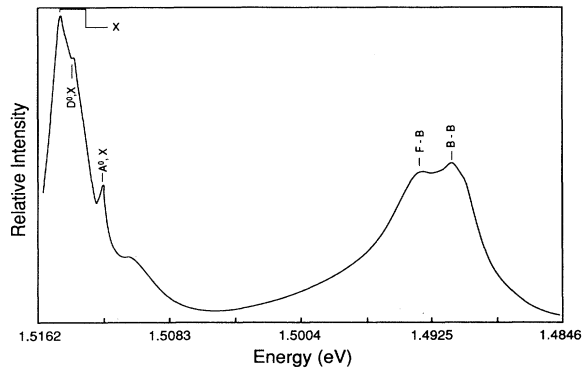

FIG. 3. Emission spectra from the sample grown by MBE.

cas are shown in the inset of Fig. 4; when the pump energy is increased to 1.4869 eV, the replica transition energies all move to higher energy by a corresponding amount. The transition at 1.4835 eV is now masked by the increased intensity of the *B-B* transition as the pump energy moves into the more intense region of the *B-B* transition. The phonon replicas are shown in Fig. 5, for a still higher pump energy where the *B-B* transition becomes more intense. With the pump energy at 1.4897 eV the phonon replicas associated with the In_{Ga} and V_{Ga} as well as the TA(X) are still observed, and in addition phonon replicas associated with TO and LO phonons are beginning to appear. With a further increase in the pump energy to 1.4924 eV, which lies between the *F-B* and *B-B* peak intensities, the phonon replicas identified with In_{Ga} and V_{Ga} are now masked by the intensity of the *B-B* transition, and only TA(X) is observed along with the LO and TO replicas of the pump energy. These are shown in the inset of Fig. 5. The phonon energies obtained from these transitions are given in Table II.

IV. THEORETICAL

Our theoretical description of assigning observed transitions to impurity vibrational modes (e.g. In_{Ga}, V_{Ga}, etc.) in GaAs consists of two parts. In the first step, we use a simple, but first-principles bond orbital model of Harrison[7] to study the lattice relaxation around the impurity atoms. The local distortions caused by substitutional impurities are determined from the minimum of total bond energy. Values of the radial force constant at the impurity site are then evaluated approximately from the second derivative of the bond energy. In the second step, the frequencies of the impurity vibrations are obtained by using a Green's function theory.[8]

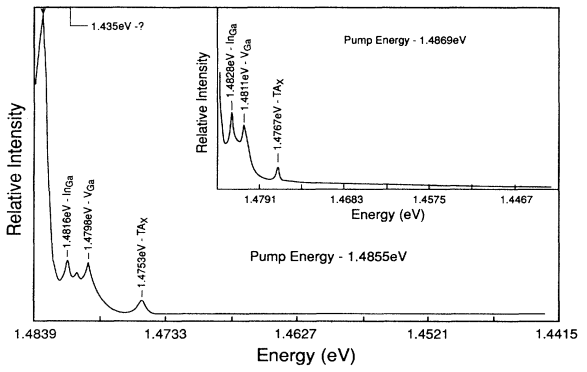

FIG. 4. Phonon sidebands associated with the emission spectra from Fig. 3 with pumping energies at 1.4855 eV, and at 1.4869 eV in the inset.

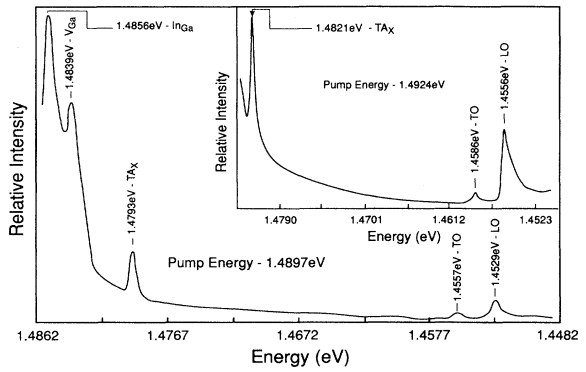

FIG. 5. Phonon sidebands associated with the emission spectra from Fig. 3 with pump energies at 1.4897 eV, and at 1.4924 eV in the inset.

In setting up the dynamical matrix in the Green's-function formalism, we evaluate all the involved Greens-function matrix elements ($\mathbf{G}^0$) numerically by incorporating phonons generated by an 11-parameter rigid-ion model fitted to the inelastic neutron-scattering data of GaAs. The nearest-neighbor force-constant changes caused by defects are properly included in the perturbation matrix ($\mathbf{P}$), and the frequencies of the impurity modes are determined by setting the determinant of the dynamical matrix equal to zero $\{\mathrm{Re}|\mathbf{I}-\mathbf{G}^0\mathbf{P}|=0\}$.

For a substitutional defect in a zinc-blende host crystal such as GaAs, the point group is T_d. If the impurity-host interaction is confined to the nearest-neighbor (nn) atoms, the (15×15) size Green's-function and perturbation matrices can be expressed conveniently in the basis of symmetry coordinates. The 15-dimensional irreducible representation Γ of T_d (Γ_{T_d}) symmetry expressed in terms of Cartesian coordinates can be reduced to $\Gamma_{T_d} = A_1+E+F_1+3F_2$. The A_1 coordinate consists of a "breathing-type" motion in which the impurity atom remains stationary while the nn host atoms move radially. In the F_1 and E coordinates, the impurity remains at rest, and the nn atoms move. It is worth mentioning that only in the triply degenerate FG_2 (IR and Raman active) mode the impurity vibrates. Therefore, we expect localized vibrational modes (LVM's) beyond the maximum phonon frequency ω_m of the host lattice, with F_2 representation for light impurities occupying either the Ga or As site in GaAs. For heavier impurities (e.g., In_{Ga}), on the other hand, we expect in-band modes to occur for each type of vibration if force-constant variations between the impurity and its nn are appropriately included. Such modes will not be easily detected if their frequencies lie in the region where the density of lattice phonons is

TABLE II. Phonon replicas along with their experimentally determined and calculated energies obtained using different pump beam energies. * refers to this work.

Pump energy (eV)	TA(X) (meV) Expt.*	Calc	V_{Ga} (meV) Expt.*	Calc	In_{Ga} (meV) Expt*	Calc	? (meV)	LO (meV) Expt.*	Calc	TO (meV) Expt.*	Calc
1.4855	10.2	10.2	5.7	5.1 A_1	3.9	4.4 F_2 25.0 A_1	2.0		36.7		33.9
1.4869	10.2		5.8		4.1						
1.4897	10.4		5.8		4.1			36.8		34	
1.4924	10.2							36.8		33.8	

high. However, if the impurity vibrates at a frequency where the density of states is low, such in-band resonance modes can be easily detected.

The solution of dynamical matrix $\{\mathrm{Re}|\mathbf{I}-\mathbf{G}^0\mathbf{P}|=0\}$ with appropriate force perturbation for In_{Ga} provides no LVM in the F_2 irreducible representation. However, several in-band modes of A_1 and F_2 representations are predicted. Green's-function calculation for an ideal Ga vacancy is also performed in which the V_{Ga} is modeled simply by removing interactions with the missing Ga atom and leaving all other atoms at perfect lattice sites. Theoretical results of in-band modes reported in Table II for In_{Ga} and V_{Ga} compare favorably with the observed impurity-induced features. The V_{Ga}-related breathing mode near 6 meV in GaAs has also been observed recently by Raman spectroscopy.[9] We are unable to establish the identity of the observed impurity mode near $\sim$2 meV. It is likely that this mode is related to a complex center involving In_{Ga}.

V. CONCLUSION

The emission spectra from high-purity GaAs is rich in phonon structure. The phonons couple strongly to the free exciton with somewhat weaker coupling to the donor-bound exciton. Coupling occurs at all of the major symmetry points in **k** space. Only intrinsic phonon structures are observed, showing high-quality material as also determined by independent electrical and optical measurements. The sample containing the higher impurity concentration with associated defects does not exhibit the intrinsic phonon structures observed in the high-purity sample. In this sample extrinsic phonon structure is observed that can be identified with impurities and defects present in the sample. The difference in the material quality of the two samples is clearly distinguished in the resulting phonon spectra associated with their optical transitions. This characterization technique in conjunction with supplementary techniques provides additional information for evaluating material quality.

ACKNOWLEDGMENTS

The authors would like to thank J. E. Ehret and E. N. Taylor for crystal-growth support, T. A. Cooper for electrical measurements, and C. W. Litton for technical support. The work of D.C.R. and D.C.L. was performed at Wright Laboratory, Solid State Electronics Directorate (WL/EL), Wright Patterson Air Force Base, OH under U.S.A.F. Contract No. F33615-91C-1765. The work of D.N.T. was supported by the National Research Council.

*Permanent address: Department of Physics, Indiana University of Pennsylvania, Indiana, PA 15705-1087.

[1]W. Cochran, S. J. Fray, A. Johnson, J. E Quarrington, and N. Williams, J. Appl. Phys. **32**, 2102 (1961).

[2]See for example, K. Kunc, Ann. Phys. (Paris) **8**, 319 (1973); C. Patel, T. J. Parker, H. Jamshidi, and W. F. Sherman, Phys. Status Solidi B **122**, 461 (1984).

[3]J. L. T. Waugh and G. Dolling, Phys. Rev. **132**, 2410 (1963).

[4]G. Dolling and J. L. T. Waugh, in *Lattice Dynamics*, edited by R. F. Wallis (Pergamon, London, 1965), p. 19.

[5]T. Sekine, K. Vchinokura, and E. Matsuura, J. Phys. Chem. Solids **38**, 1091 (1977).

[6]H. Fröhlich and N. F. Mott, Proc. R. Soc. London Ser. A **171**, 496 (1939).

[7]W. A. Harrison, *Electronic Structure and the Properties of the Solids* (Freeman, San Francisco, 1980).

[8]D. N. Talwar, M. Vandevyver, K. K. Bajaj, and W. M. Theis, Phys. Rev. B **33**, 8525 (1986).

[9]T. Sauncy, M. Holtz, and R. Zallen, Bull. Am. Phys. Soc. **39**, 149 (1994).